A Semiempirical Quantum Chemical Study of Some Local Aspects of Ionic Conduction in Poly(ethylene oxide): Ion Motion and Rotational Barriers

Vladimiro Mujica,*,† Manuel Malaver,†,‡ and Fernando Ruette*,‡

Escuela de Química, Facultad de Ciencias, Universidad Central de Venezuela, Apartado 47102, Caracas 1020-A, Venezuela, and Centro de Química, Instituto Venezolano de Investigaciones Científicas, I.V.I.C., Apartado 21827, Caracas 1020-A, Venezuela

Received: December 5, 1997; In Final Form: May 13, 1998

Several aspects of electronic potential energy curves for the ionic conduction process in poly(ethylene oxide) are modeled. A supermolecule is taken as a local model for a section of a polymer chain in the amorphous phase. Ion-polymer interaction, rotational barriers for the free and charged supermolecule, and the activation energy for intrachain ionic motion were calculated. For the latter, the oxygen-cation distance is considered as the reaction coordinate. The supermolecule assembly consists of five monomer units and a proton as probe ion. Strong coupling occurs between the motion of the ion and the flexional dynamics of the polymer that is manifest in the rearrangement that takes place in the nuclear framework of the chain as the position of the ion changes. The calculated activation energy was found in the range of the experimental values. All these results are consistent with the picture that ionic conduction in solid electrolytes such as poly(ethylene oxide) takes place mainly in the amorphous phase, because a considerable degree of flexibility on the polymer backbone is required to allow for the necessary bond rearrangements to promote cationic motion.

I. Introduction

A great deal of the interest in polymer electrolytes is due to their potential applications in batteries,[1a−d] capacitors,[1e] artificial muscle,[1f] and electrochromic devices.[1g] Several reviews and articles[2] deal with the transport properties of these materials.

There is extensive experimental evidence that conduction in ionic conductors, such as poly(ethylene oxide) (PEO), involves a strong coupling between the flexional dynamics of the polymer backbone and the ionic motion.[3] Perhaps the strongest such evidence is the finding that the conductivity drops dramatically for temperatures below the equilibrium glass transition temperature (T_g). Both NMR relaxation and fast-quenching studies indicate that the amorphous phase seems to be crucial for conduction to occur.[3c,4] Motion of the polymeric chain in the amorphous phase creates the necessary conditions for ionic motion to occur. This motion is energetically hindered in the crystalline phase because of the high rotational barriers involved.

Semiempirical methods have become increasingly popular for the study of complex molecular systems because of their ability to handle a large number of electrons.[5] Standard choice of parameters for the Hamiltonian prevents, in a way, the kind of systematic improvement that can be achieved with a multiconfigurational or perturbational procedure. This disadvantage is compensated to some extent by working within a given "chemical family" in which the same set of semiempirical parameters can be used for all the members of the family. However, recent formalism has shown that parametric model Hamiltonians (semiempirical Hamiltonians) can achieve systematic improvements, using algorithms based on simulation techniques.[6] In general, semiempirical methods have proven most useful in revealing trends for chemical behavior[5a,6b] and for analyzing electronic potential energy surfaces.[7]

We have used the semiempirical program AMPAC[8] to study some local aspects of the potential energy surface of PEO and of the ion $PEOH^+$ that could be relevant to understanding the nature of the conduction process. The study was performed without imposing translational symmetry, because we were interested in a local defect represented by the presence of the charge. Rotational barriers for the neutral and the charged system were studied using a supermolecule formed by five monomer units. Ionic motion was analyzed through the construction of energy-reaction coordinate curves, where the reaction coordinate was taken as a typical oxygen-proton distance, whereas allowance was made for full energy optimization of the remaining internal coordinates.

The model attempts to represent the motion of the ion in a section of a polymer chain in the amorphous phase. In addition to understanding the local aspects of ion motion addressed in this work, a description of the conduction process would require an adequate treatment of disorder in the amorphous phase which is beyond the scope of this article.

The organization of this article is as follows: Section II is devoted to a brief account of the relevant experimental information about PEO and its salts and to a description of the theoretical model. Section III contains the results about the energetics of rotation for the neutral and charged systems, ion−polymer interaction ion-motion barrier, and motion mechanism. Finally, Section IV presents some conclusions and considerations about further work on the subject.

II. Description of the System and Model

PEO is a partially crystalline material with a crystalline phase that accounts for approximately 60% of the ambient temperature volume. It has a glass transition temperature of 213 K.[9]

Ion transport in amorphous PEO salt complexes is believed to occur through the relative motion of polymer chain segments,

* To whom all correspondence should be addressed.
† Universidad Central de Venezuela.
‡ Instituto Venezolano de Investigaciones Científicas.

10.1021/jp980446q CCC: $18.00
Published on Web 12/17/1998

involving an associative/dissociative process between the mobile ion and some backbone atoms. For positive ions, as we are considering here, the ion-backbone interactions will be predominantly between the oxygen atoms and the proton. For temperatures below T_g, the conductivity is expected to drop very rapidly, as chain mobility is reduced drastically.

A simple phenomenological model that accounts for the dependence of the conductance (σ) on the temperature (T) is given by the Vogel-Tamang-Fulcher equation[10]

$$\sigma = AT^{-1/2} \exp(-E_a/k_B(T - T_g)) \qquad (1)$$

where k_B is the Boltzmann constant, E_a is an energy parameter which formally has units of activation energy, and A is a constant for each material.

Because ion transport in a polymer is a complex process that involves nuclear motion in the presence of multiple potential barriers, it cannot be assigned a single activation energy as in a conventional Arrhenius-activated process. This deviation from Arrhenius behavior is reflected in eq 1. However, the parameter E_a in this equation gives some idea about the energy involved in the ion motion, and it has been reported for several polyethers with alkali metal salt complexes.[1b,3b,11] These pseudoactivation energies range from a low value of about 0.35 eV up to 2 eV. For NaSCN·4PEO a value of E_a of approximately 0.61 eV would result for a dissociative transport process involving the breaking of one sodium−oxygen bond, whereas it is expected to be larger than 1.3 eV if two sodium−oxygen bonds are broken.

The most widely accepted microscopic theory of diffusion in polymer electrolytes is the dynamic bond percolation (DPB) by Ratner and Shriver (see ref 2a and references therein). In this model the percolation pathways are continually redefined, and continuous long-range diffusion requires breaking of local coordination links about the cation. In an amorphous polymer the ionic diffusion depends on statistical intrachain and interchain correlated motions.

The main purpose of this article is the modeling of the ion transport along a chain represented by a supermolecule. This will enable us to establish a connection between the microscopic mechanism, the energetics of the ion motion (potential energy curves for activation), and the polymer torsion (rotational energy curves).

Theoretical Polymer Model. As stated in the introduction, we have considered a supermolecule consisting of five monomeric units of the type $-(CH_2)_2-O-$ which yields the molecular formula $HC_{10}H_{20}O_5H$. For the ionic supermolecule, the species $C_{10}H_{20}O_5H_2+$ was chosen.

Our basic justification for using the supermolecule model is to provide a molecular framework that is flexible enough to permit the kind of distortions that occur in the amorphous phase during ion transport and that are hindered in the crystalline phase. In addition, bond breaking associated with ionic motion through the polymeric backbone is mostly a local effect involving a small number of bonds at the time, and for this purpose the chosen number of five units in the supermolecule seems to be adequate. Support for this local model is also derived from molecular dynamics calculations.[12]

There is another reason for considering a finite molecular structure instead of an extended solidlike system: the suppression of the translational symmetry allows us to represent the charge in the ionic supermolecule as a local defect. The use of translational symmetry would place a charge in each repeated unit cell, thereby creating spurious symmetric coupled interactions between the charges.

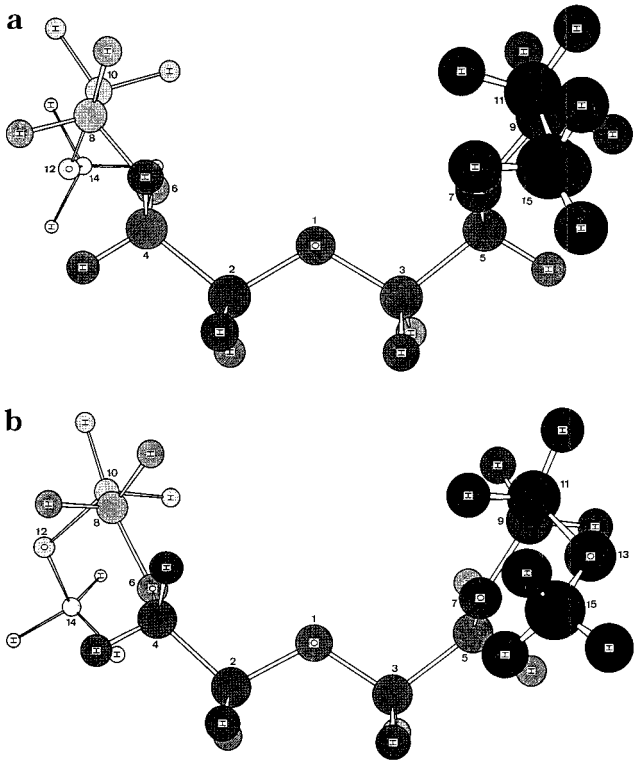

Figure 1. Optimized geometry for the polymer: (a) the gaseous phase; (b) the crystalline phase.

We have considered a hydrogen ion (a proton) as the simplest possible representative of the heavier and more complex positive ions involved in real salts. From the point of view of an electronic structure calculation, this simply amounts to including an extra atom in the system at a given position. Polymer electrolytes that transport protons also have been reported in the literature[2a,13,1g]

III. Results and Discussion

The semiempirical AMPAC package,[8] which includes codes for AM1,[14] MINDO/3,[15] and MNDO[16] was used to perform molecular orbital calculations for the electronic structure of the neutral and ionic supermolecule. The results reported in this article were obtained using the MNDO method.

Geometry. We performed an energy optimization to find the equilibrium geometry of the neutral supermolecule. The resulting geometry is displayed in the structure of Figure 1a. This should be compared with the structure depicted in Figure 1b which corresponds to the crystalline phase. It was obtained through the same optimization procedure, but imposing translational symmetry. In both cases, the initial geometry for the optimization procedure was taken as that of PEO in crystalline phase based on X-ray diffraction.[17] These figures also provide the atomic labels considered throughout this article. Both structures show a characteristic helical geometry; most of the variation from one phase to the other goes into small changes in the interatomic distances and angles.

Energy minimization for the isolated supermolecule, with the structure of the solid as a starting point, leads, in principle, to the local minimum closest to the crystal structure. Whether this minimum is the global one for the gas phase deserves further investigation using an ab initio methodology. However, the important point here is whether the supermolecule is a reasonable model for a chain in the amorphous phase. X-ray studies of many amorphous materials indicate short-range order similar

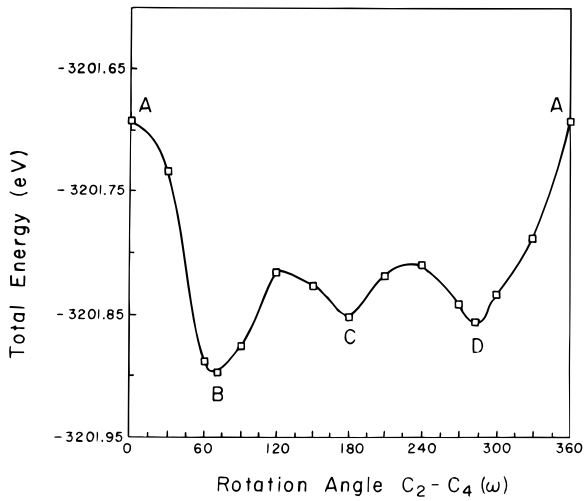

Figure 2. Energy profile for the rotation of the C_2-C_4 bond in poly(ethylene oxide).

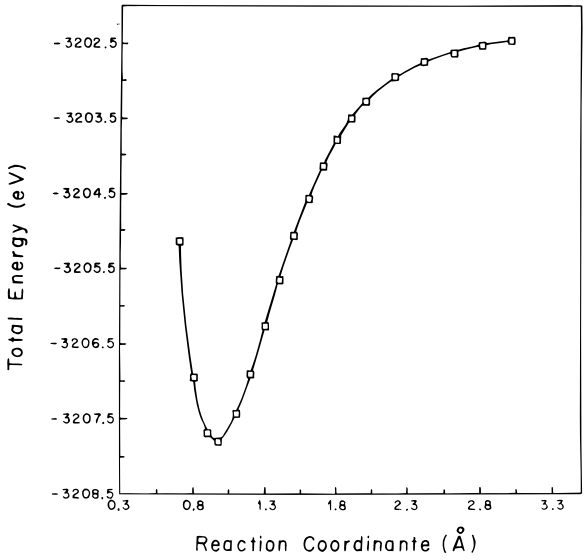

Figure 3. Potential energy curve for docking of the ion (H^+) on the O_1 adsorption site.

to the solid but absence of long-range order. In addition, as stated in Section II, experimental evidence about ion transport indicates a considerable degree of flexibility for the molecular units in the amorphous phase. Both of these basic features are present in the model we are proposing.

Rotational Barriers for the Neutral Supermolecule. We have considered rotations around the C_2-C_4 bond in the supermolecule and constructed the corresponding energy profiles as a function of the dihedral angle (ω) defined with respect to the less stable configuration. This profile is shown in Figure 2. In principle, this figure should be symmetric with respect to the value $\omega = 180°$. The deviation from this symmetry should be taken as a numerical error that is related to the fact there are many close-lying local minima in the potential energy surface of the supermolecule.

The value $\omega = 0°$ (labeled as A in Figure 2) corresponds to a maximum of energy, in which atoms 1 and 6 are facing each other in an eclipsed configuration. As ω increases, the steric hindrance between pairs of oxygen and hydrogen atoms diminishes, until the minimal energy configuration is achieved ($\omega = 71°$). This value is close to the experimental equilibrium dihedral angle in the crystalline phase ($\omega = 65°$). The two extreme positions (points A and B on the curve) are separated by about 0.21 eV, which is associated with the total rotational barrier. Smaller barriers associated with changes between intermediate configurations B→C and C→D (about 0.08 and 0.04 eV, respectively) are also observed. Calculated barriers fall within the range 0.04−0.31 eV corresponding to reported rotational barriers for extended polymers, such as polyethylene.[18]

Ion-Polymer Interaction. To study the interaction of a cation with the polymeric chain, the potential energy curve was constructed by bringing a H^+ ion, as the simplest example, toward the central oxygen (O_1). The results, as expected, reveal an attractive interaction, as shown in Figure 3. In this case, the polymer geometry was considered fixed at the equilibrium configuration, and an optimal $O-H^+$ distance of 0.97 Å was found. This value is close to that reported for OH and OH^+ molecules (0.97 and 1.03 Å, respectively[19]). A longer cation-polymer distance should be expected, but our model does not include the anion. The ion adsorption leads to a stabilization of the system of about 6.4 eV, which is very high, due to the absence of the anion.

The net charge on the ion is redistributed in the polymer: the ion charge +1.0 lowers to +0.32 au and the O_1 decreases its charge from −0.35, in the neutral polymer, to −0.12 au; i.e., $\Delta q(O_1) = 0.23$ au ($\Delta q(X)$ is defined as the charge difference on X atoms between neutral and charged systems). The rest of the charge is distributed on the neighbor C_2, C_3, C_4, and C_5 atoms ($\Delta q(C) = 0.07$ au) and near hydrogen atoms ($\Delta q(H) = 0.38$ au). This last feature shows that hydrogens close to the ion adsorption site become more acidic.

Keeping the equilibrium bond distance H^+-O_1 fixed, the optimization of the polymer chain was carried out. A comparison of the polymer geometry with and without charge (see Figures 1a and 4) reveals that the system is reorganized. Distances between the ion and oxygen atoms $D(H^+-O)$ are reduced as shown by ΔD (defined as the interatomic distance between the neutral and the charged species) values for H^+-O_6, H^+-O_7, H^+-O_{12}, and H^+-O_{13} of −0.25, −0.12, −1.02, and −0.76 Å, respectively. This is a consequence of Coulomb interactions of the electronic densities on oxygen atoms and the remaining positive charge of the adsorbed ion. Thus, the oxygen clustering around the positive charge forces a twist of all the molecular backbone, i.e., a solvation-like effect of the cation. The same trend is found in the crystal structure of PEO_3-NaI.[20] Ratner and Shriver[2a] also proposed a similar effect in which ion transfer is assisted by four oxygen atoms.

Ion-Motion Barriers. The calculations of the barrier for ion motion and the description of the geometrical rearrangement that takes place in the supermolecule backbone are probably the most important aspects of our study. This rearrangement is caused mostly by rotations around single bonds that tend to move the oxygen atoms around the proton. The distance between the proton and O_1 was chosen as reaction coordinate.

As starting geometry, we take the one depicted in Figure 4, which places the H^+ ion at a distance of 0.97 Å from O_1. This geometry was obtained carrying out a vertical docking of H^+ on O_1 and thereafter optimizing the geometry. We have constructed the energy profile corresponding to the process of increasing the distance H^+-O_1 and optimizing the geometry at each step. The results are displayed in Figure 5.

The first important aspect to notice is the increase in energy as H^+ is moved further from O_1, starting from a value of 0.9 Å, until it reaches a maximum at a distance of 1.38 Å. Thereafter, a sharp energy decrease is observed for a variation of only 0.1 Å. An analysis of the geometry of the supermolecule during this process, indicates that a progressive approach of the

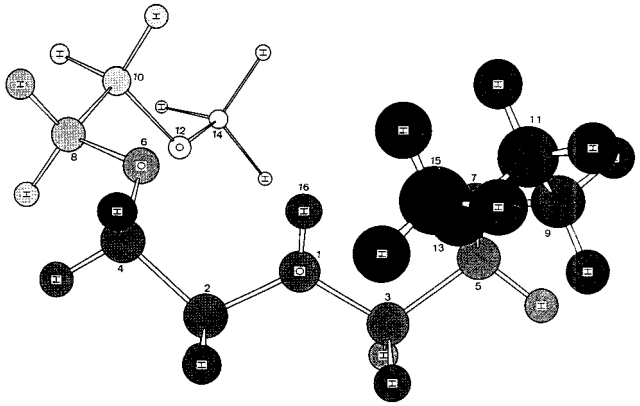

Figure 4. Geometry of the polymer with the adsorbed cation.

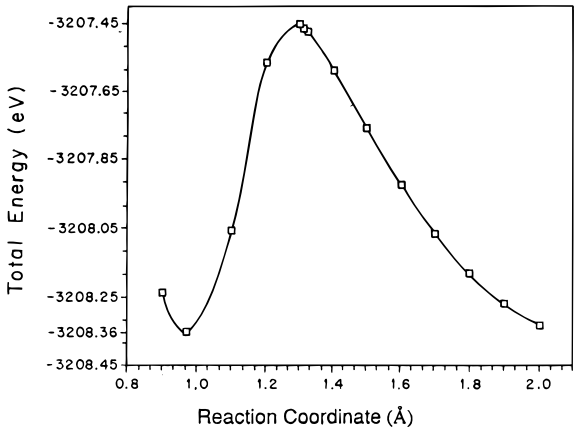

Figure 5. Calculated energy curve for ion transfer from O_1 to O_6 adsorption sites.

H^+ ion to O_6 is taking place and that the drop in energy corresponds to the capture of the ion by O_6. The capture proceeds until the distances H^+-O_1 and H^+-O_6 are 2.0 and 0.98 Å, respectively. The nature of the ion transport will be analyzed in more detail in the next section. We just mention here that the same type of energy profile is obtained starting from the configuration where H^+ is attached to O_6 and then it is displaced toward O_7 and that the motion barrier is of the order of 0.93 eV in either case.

It is worth observing that the presence of several electronic states in the neighborhood of the maximum in Figure 5 makes it difficult to obtain a smooth potential energy curve. This is caused by the computational procedure used in the energy calculation, because the initial guess for the density matrix at each iteration is taken from the previous geometry. This forces the supermolecule to continue in the same electronic state beyond the maximum until an acute energy variation occurs as a consequence of a change in the electronic state. To correct this situation we performed a series of calculations in which the initial guess for the density matrix was taken for geometries to the right and to the left of the maximum. This kind of situation has been found in other instances where bond-breaking and curve-crossings associated with two different electronic states are reported, e.g., H_2 dissociation on a Ni model surface.[7c] The calculated barrier found here (0.93 eV) is in the range of experimentally reported pseudoactivation energies (0.35−2.0 eV).[10] Recently, Chandra et al.[21] found values of about 0.85 eV for almost crystalline PEO:NH_4SCN films. However, for the amorphous polymer; i.e., above the phase transition temperature, the activation parameters are substantially lower (0.30−0.37 eV).

Motion Mechanism. Figure 6 shows four snapshots of the transfer of H^+ from O_1 to O_6. The first view (a) corresponds to the supermolecule with H^+ attached to O_1 and the important point is the geometric distortion with respect to Figure 1a, as shown in Figure 4. As the process advances (H^+ moves away from O_1), there is a clear three-dimensional twist of the molecular backbone, pictured in Figure 6b, with O_1, O_6, O_{12}, and O_{13} assisting the transfer process. These have the highest ΔD, with a larger participation of the former two. Figure 6c shows the transfer transition complex, and in Figure 6d the transfer has been completed.

To gain further understanding about the mechanism of ion transfer from O_1 to O_6, the variation of s−s and s−p overlap integrals for the O_6-H^+ bond; the charge density on H^+, O_1, and O_6, and the total energy are presented in Table 1 for selected values of the reaction coordinate, $r(O_1-H^+)$. As the cation moves away from O_1, the electronic density increases on O_1 and the positive charge grows on the cation. A very small addition in the electronic density on O_6 is observed due to inductive effects caused by the increase of electronic charge to the O_1 atom. Instability starts growing until a value of $r(O_1-H^+)$ of about 1.3 Å is reached. At this point, a O_6-H bond starts building up as shown by the increase in the s−s and s−p overlap integrals. There is a concomitant decrease in the H^+ charge because charge density from O_6 begins to be transferred and correspondingly, the electronic density on O_1 grows due to the charge flow from the cation. The system reaches a new point of stability for a value of $r(O_1-H^+)$ of 2.00 Å that corresponds to a $r(O_6-H^+)$ of about 0.98 Å.

Some conclusions might be inferred from stages of the $O_1...H^{+\cdots}O_6$ bond formation. There is a correlation between the overlap integrals and the energy of the system: higher overlap population implies more stable system. Therefore, it is expected that bigger cations (e.g., Na^+ has longer ionic radii and therefore more diffuse orbitals) would present a more stable transition state because the overlap between the cation and the bridge adsorption site (O_1-O_6) would be higher. Note also that the bending vibration of $O_1-C_2-C_4-O_6$ frame would also have influence in the height of the activation barrier. There are situations in which the $O_1...O_6$ distance decreases, allowing stronger $O_1...H^{+\cdots}O_6$ interactions. Therefore, temperatures above the transition phase temperature (T_g) will produce polymer distortions that will lead to a more effective ion transfer. This issue was not considered here.

Rotational Barrier in the Charged Polymer. An important issue in the ion motion process is the change in the activation barrier due to the rotational barrier for the charged complex, as the reaction coordinate changes. The distance O_1-H is artificially maintained constant. Table 2 shows the value of the rotational barrier for selected values of the reaction coordinate $r(O_1-H^+)$. These values correspond to rotations about the C_2-C_4 bond, and they were obtained in a way similar to that described for rotational barriers in the uncharged supermolecule.

For short $r(O_1-H^+)$ distance, 0.97 Å, the rotational barrier (about 0.26 eV) is slightly higher than that of the uncharged polymer (0.21 eV). For intermediate $r(O_1-H^+)$ distances, the barrier increases, achieving a maximum value of 0.87 eV at $r(O_1-H^+) = 1.3$ Å that corresponds to the formation of the ion transfer complex ($O_1...H^{+\cdots}O_6$). The increase in the barrier is obviously related to the fact that rotation implies breaking of partial $O_1...H^+$ and $O_6...H^+$ bonds.

Because rotation is necessary to rearrange the oxygen atoms involved in the transfer, we conclude that rotational barriers in

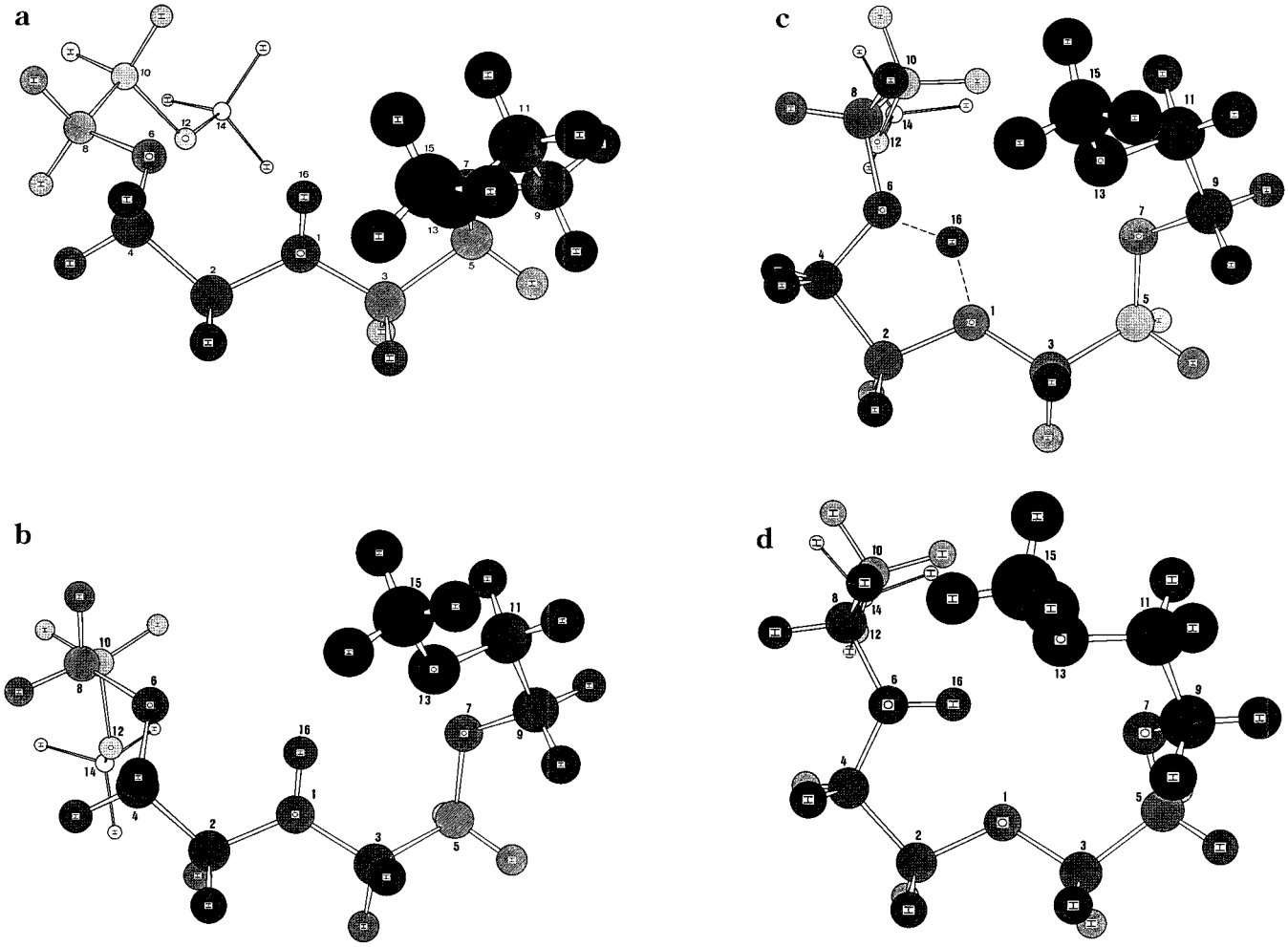

Figure 6. Geometries of the supermolecule at different stages of the ion transfer from O_1 to O_2. (a) Starting configuration; (b) distorted structure; (c) transition state; (d) ion transferred to O_6.

TABLE 1: Overlap Integrals for O_6-H^+ Bond; Charge on H^+, O_1, and O_6; and Total Energy as a Function of the Reaction Coordinate Corresponding to the Motion of the Ion H^+ from O_1 to O_6

$r(O_1-H^+)$ (Å)	overlap integrals O_6-H^+		charge (au)			total energy (eV)
	s-s	s-p	H^+	O_1	O_6	
0.90	0.001	0.002	+0.327	−0.114	−0.381	−3208.23
0.97	0.001	0.003	+0.355	−0.138	−0.383	−3208.36
1.20	0.003	0.006	+0.459	−0.201	−0.395	−3207.57
1.30	0.184	0.220	+0.386	−0.339	−0.263	−3207.46
1.35	0.208	0.251	+0.383	−0.358	−0.239	−3207.51
1.40	0.245	0.290	+0.375	−0.371	−0.212	−3207.59
1.70	0.331	0.413	+0.359	−0.401	−0.152	−3208.07
2.00	0.360	0.451	+0.355	−0.394	−0.142	−3208.34

TABLE 2: Rotational Barriers for Rotations Around the C_2-C_4 Bond in the Charged Supermolecule for Selected Values of the Reaction Coordinate

O_1-H^+ distance (Å)	rotational barrier (eV)
0.97	0.26
1.10	0.31
1.20	0.40
1.30	0.87

the uncharged and charged species are not substantially different, except when bond breaking is involved. This situation is not relevant until the proton-transfer process has advanced to the formation of the transfer intermediate. Once it is formed, the rotation through C_2-C_4 will decrease the energy of the system, see point A in Figure 2. It corresponds to the eclipsed configuration in which the intermediate complex is formed. At this point, the anion will change its location accordingly with the direction of the electric field. To reach this situation, a substantial amount of thermal activation is necessary to overcome a rotational barrier of about 0.26 eV and an activation energy of around 0.93 eV to form the transfer intermediate ($O_1...H^{+}...O_6$) in the supermolecule. The value obtained seems somewhat high, but the qualitative trend appears to be correct and the results show that the coupling between the rotational dynamics and the ion motion mechanism is of vital importance for the conduction.

IV. Conclusions

The results reported here confirm the idea that intramolecular ionic transport involves a strong coupling of the flexional and rotational dynamics with ion motion. Using a proton as probe, a description of the intrachain conduction emerges in which four oxygen atoms assist the proton-transfer process, distorting the helical three-dimensional array of the supermolecule.

The important energy barriers for rotation and motion indicate that some amount of thermal activation is required. This confirms the conjecture that the amorphous phase that exists for temperatures above the glass transition is of primary importance for the conduction process. It is also consistent with the observation that amorphous polymers with flexible back-

bones, that have low T_g, show the highest ambient-temperature conductivity. Examples include solixane and phosphazene comb polymers.

Further work should include the study of the potential energy surfaces for more realistic cations with the corresponding anions and a higher level of accuracy in the description of the electronic structure. A better understanding of interchain ion motion using a similar model to that described in this paper for the intramolecular process, should also be of value. Other models for this process, based on ideas of dynamic disorder motion in a lattice, have been worked out by Lonergan and co-workers,[22] who suggest that the conductivity of polymer electrolytes is diffusion dominated and that ion−ion interactions play an important role.

Finally, developing a comprehensive model for conduction would require a reasonable description of disorder in the amorphous phase in conjunction with the local aspects of ion motion considered in this article. This is an ambitious program which shares all the difficulties with other physical problems dealing with transport in disordered structures.

Acknowledgments. Funding for this research was provided by CDCH-UCV (Caracas, Venezuela). V.M. would like to thank Prof. Mark Ratner, from Northwestern University, for his sharp criticisms and remarks about the original version of this article, which helped improve it substantially.

References and Notes

(1) Gauthier, M.; Fauteux, D.; Vassort, G.; Belanger, A.; Duval, M.; Recoux, P.; Chabagno, J. M.; Muller, D.; Rigaud, P.; Armand, M. B.; Deroo, D. *J. Electrochem. Soc*. **1985**, *132*, 1333. (b) Armand, M. B.; Chabagno, J. M.; Duclot, M. J. K. In *Fast Ion Transport in Solids*; Vashishta, P. M.; Mundy, J. N.; Shenoy, G. K., Eds.; North-Holland: Amsterdam, 1979; p 131. (c) Bonino, F.; Ottaviani, M.; Scrosati, B.; Pistoria, G. *J. Electrochem. Soc*. **1988**, *135*, 12. (d) Fauteux, D.; Massucca, A.; McLin, M.; Van Buren, M.; Shi, J. *Electrochim. Acta* **1995**, *40*, 2185. (e) Ishikawa, M.; Ihara, M.; Morita, M.; Matsuda, Y. *Electrochim. Acta* **1995**, *40*, 2217. (f) Okusaki, H.; Osada, Y. *Electrochim. Acta* **1995**, *40*, 2229. (g) Harris, C. S.; Rukavina, T. G. *Electrochim. Acta* **1995**, *40*, 1995.

(2) (a) Ratner, M. A.; Shriver, D. F. *Chem. Rev*. **1988**, *88*, 109. (b) Tonge, J. S.; Shriver, D. F. In *Polymers for Electronic Applications*; Lai, J. H., Ed.; CRC Press: Boca Raton, FL, 1899; p 157. (c) Gray, F. M. *Solid Polymer Electrolytes*; VCH: New York, 1991. (d) Bruce, P. G.; Vincent, C. A. *J. Chem. Soc., Faraday Trans.* **1993**, *89*, 3187. (e) MacCallum, J. R.; Vincenta, C. A. *Polymer Electrolyte Reviews* 1; Elsevier: London, 1987. (f) MacCallum, J. R.; Vincent, C. A. *Polymer Electrolyte Reviews* 2; Elsevier: London, 1989. (g) Chadwick, A. V.; Worboys, M. R. In *Polymer Electrolyte Reviews*, 1; MacCallum, J. R., Vincent, C. A., Eds.; Elsevier: London, 1987. (h) Vincent, C. A. *Electrochim. Acta* **1995**, *40*, 2035.

(3) Berthier, C.; Gorecki, W.; Minier, M.; Armand, M. B.; Chabagno, J. M.; Rigaud, P. *Solid State Ionics*, **1983**, *11*, 91. (b) Cheradame, H.; Souquet, J. L.; Latour, J. M. *Mater. Res. Bull*. **1980**, *15*, 1173. (c) Killis, A.; Le Nest, J.; Cheradame, H. *Makromol. Chem.* **1980**, *1*, 595.

(4) (a) Cheradame, H. In *IUPAC Macromolecules*; Benoit, H., and Rempp, P., Eds. Permagon: London, 1982. (b) Ansari, S. M.; Brodwin, M.; Stainer, M.; Druger, S. D.; Ratner, M. A.; Shriver, D. F. *Solid State Ionics* **1985**, *17*, 101.

(5) (a) Ruette, F.; Sierraalta, A.; Hernández, A. In *Quantum Chemistry Approaches to Chemisorption and Heterogeneous Catalysis*; Ruette, F., Ed.; Kluwer: Dordrecht, 1992; p 320, and references therein. (b) Thiel, W. *Tetrahedron* **1988**, *44*, 7393. (c) Kolb, M.; Thiel, W. *J. Comput. Chem*. **1993**, *14*, 775.

(6) Romero, M.; Primera, J.; Sánchez, M.; Brassesco, S.; Bravo, J.; Ruette, F. *Folia Chim. Theor. Lat.* **1995**, *XXIII*, 45. (b) Ruette, F.; Poveda, F. M.; Sierraalta, A.; Sánchez, M.; Rodríguez-Arias, E. N. *J. Mol. Catal. A* **1997**, *119*, 335. (c) Sierraalta, A.; Ruette, F. *Int. J. Quantum Chem.*, submitted for publication.

(7) Ruette, F.; Hernández, A. J.; Ludeña, E. V. *Surf. Sci*. **1985**, *151*, 103. (b) Sánchez, M.; Ruette, F.; Hernández, A. J. *J. Phys. Chem.* **1992**, *96*, 823. (c) Rodríguez-Arias, E. N.; Rincón, L.; Ruette, F. *Organometallics*, **1992**, *11*, 3677.

(8) AMPAC, Dewar Research Group, University of Texas: Austin, Texas, 1985.

(9) (a) Wright, P. V.; Lee, C. C. *Polymer* **1982**, *23*, 681. (b) Neat, R.; Glasse, M.; Linford, R.; Hooper, A. *Solid State Ionics* **1986**, *18/19*, 1088.

(10) (a) Vogel, H. *Phys. Z.* **1921**, *22*, 645. (b) Tammann, V. G.; Hesse, W. *Anorg. Allg. Chem.* **1926**, *156*, 245. (d) Fulcher, G. S. *J. Am. Ceram. Soc.* **1925**, *8*, 339.

(11) Papke, B. L.; Ratner, M. A.; Shriver, D. F. *J. Electrochem. Soc.* **1982**, *129*, 1694.

(12) (a) Boinske, P. T.; Curtiss, L.; Halley, J. W.; Lin, B.; Sutjianto, A. *J. Comput.-Aided Mater. Des.* **1996**, *3*, 385. (b) Neyertz, S., Comprehensive Summaries of Uppsala Dissertations from the Faculty of Science and Technology 100. Ph.D. Thesis, Acta Universitatis Upsaliensis, Uppsala 1995.

(13) Slade, R. C. T.; Hardwick, A.; Dickens, P. G. *Solid State Ionics* **1983**, *9/10*, 1053.

(14) Dewar, M. J. S.; Zoebish, G. E.; Healy, E. F.; Stewart, J. P. *J. Am. Chem. Soc.* **1985**, *107*, 3902.

(15) Bingham R. C.; Dewar, M. J. S.; Lo, D. H. *J. Am. Chem. Soc.* **1975**, *97*, 1285.

(16) Dewar, M. J. S.; Thiel, W. *J. Am. Chem. Soc.* **1976**, *99*, 4899.

(17) Takahashi, Y.; Tadokoro, H. *Macromolecules* **1973**, *6*, 672.

(18) Tanaka, K.; Yamabe, T. *Adv. Quantum Chem.* **1985**, *17*, 251.

(19) Gray, H. B. *Electrons and Chemical Bonding*, W. A. Benjamin: New York, 1965; p 84.

(20) Chatani, Y.; Okamura, S. *Polymer* **1987**, *28*, 1815.

(21) Srivastava, N.; Chandra, A.; Chandra, S. *Phys. Rev. B* **1995**, *52*, 225.

(22) Lonergan, M. C.; Shriver, D. F.; Ratner, M. A. *Electrochim. Acta* **1995**, *40*, 2041.